Report

Nord2000. Comprehensive Outdoor Sound Propagation Model. Part 2: Propagation in an Atmosphere with Refraction

Client: Nordic Noise Group & Nordic Road Administrations

AV 1851/00
Page 1 of 50

31 December 2000
Revised 31 December 2001
Revised 31 March 2006

DELTA
Danish Electronics,
Light & Acoustics

Venlighedsvej 4
2970 Hørsholm
Danmark

Tlf. (+45) 72 19 40 00
Fax (+45) 72 19 40 01
www.delta.dk

Title
Nord2000. Comprehensive Outdoor Sound Propagation Model. Part 2: Propagation in an Atmosphere with Refraction

Journal no.	**Project no.**	**Our ref.**
AV 1851/00	A550054	BP\JK\lm

Client
Nordic Noise Group & Nordic Road Administrations

Summary

See page 8

DELTA, 31 March 2006

Birger Plovsing
Noise & Vibration

Contents

List of Symbols

j	Complex unit ($=\sqrt{-1}$)
f	Frequency (at the centre frequency in case of 1/3 octave bands)
k	Wave number ($=2\pi f/c \quad =2\pi/\lambda$)
ω	Angular frequency ($=2\pi f$)
c	Speed of sound ($=20.05\sqrt{t+273.15}$)
λ	Wave length ($=c/f$)
L	Sound pressure level
L_W	Sound power level
A, B, C	Constants in a sound speed profile with a logarithmic and linear part
ΔL	Propagation effect (ΔL = -Attenuation)
ΔL_d	Propagation effect of spherical divergence
ΔL_a	Propagation effect of air absorption
ΔL_t	Propagation effect of terrain (ground and barriers)
ΔL_s	Propagation effect of scattering zones
ΔL_r	Propagation effect of reflecting obstacle
p	Complex pressure
p_{diffr}	Complex pressure from a diffracted path
p_0	Complex pressure from free field wave
α	Phase angle
x, y, z	Spatial coordinates
P	Point (1-D, 2-D and 3-D)
d	Horizontal distance
h	Vertical height
h_S	Height of source above local ground
h_R	Height of receiver above local ground
R	Distance between to points
ℓ	Path length
$\Delta\ell$	Path length difference
θ	Angle (of incidence or diffraction)
ψ_G	Grazing angle (=π/2-θ)
S	Surface area
β	Wedge angle
Q	Spherical wave reflection coefficient
$\Re_p$	Plane wave reflection coefficient

$\Re$	Pressure-amplitude reflection coefficient based on the random incidence absorption coefficient
ρ_E	Energy reflection coefficient (= $\|\Re\|^2$)
Z	Acoustic impedance (normalised, specific)
σ	Flow resistivity
σ_r	Roughness parameter
D	Diffraction coefficient
R_{ve}	Transmission loss from diffraction of a vertical edge
F_λ	Fraction of the wavelength (used in determination of Fresnel zones)
w	Fresnel-zone weight
F	Fraction of coherent sound
F_f	Fraction of coherent sound, frequency band averaging
$F_{\Delta\tau}$	Fraction of coherent sound, fluctuating refraction
F_c	Fraction of coherent sound, partial coherence
F_r	Fraction of coherent sound, surface roughness
F_s	Fraction of coherent sound, scattering zones
u	Average wind speed component in the direction of propagation
σ_u	Standard deviation of the wind speed component in the direction of propagation
t	Temperature in °C
dt/dz	Average temperature gradient
$\sigma_{dt/dz}$	Standard deviation of the temperature gradient
z_0	Roughness length
τ	Travel time along a sound ray
C_v^2	is the turbulence strength corresponding to wind
C_T^2	is the turbulence strength corresponding to temperature
$\Delta c/\Delta z$	Gradient of equivalent linear sound speed profile
ξ	Relative gradient of the equivalent linear sound speed profile
c(0)	Sound speed at the ground in the equivalent linear sound speed profile
c(z)	Effective sound speed at height z above the ground

Subscripts

S	Source
R	Receiver
SCR	Screen

Functions

ln	Natural logarithm (base e)
log	Logarithm to base 10
H(x)	Heavisides' step function (H = 1 for $x \geq 0$ and H = 0 for $x < 0$)
sign(x)	Signum function (sign = 1 for $x > 0$, sign = 0 for $x = 0$, sign = -1 for $x < 0$).

Preface

This prediction method has been developed within the frame of a Nordic project, Nord2000. It would not have been possible without the generous support from authorities and research councils throughout the Nordic countries. The main financial support has come from the Nordic Council of Ministers, but additional support, both to the main project and to related projects, has come from the following organizations:

- Miljøstyrelsen, Denmark
- Danish Road Directorate
- Danish National Railways
- Ministry of the Environment, Finland
- The Finnish Road Administration
- The Norwegian Road Administration
- Norwegian State Pollution Authority
- The Swedish Rail Administration
- The Swedish Road Administration
- The National Board of Health and Welfare, Sweden
- The Swedish Transport & Communications Research Board
- Nordtest

The prediction method was developed by a joint Nordic project group consisting of Jørgen Kragh and Birger Plovsing, DELTA Danish Electronics, Light & Acoustics, Denmark, Svein Storeheier, Sintef Telecom and Informatics, Norway, and Hans Jonasson, Mikael Ögren and Xuetao Zhang, SP Swedish National Testing and Research Institute. Juhani Parmanen, VTT Building Technology, Finland has been an observer.

The support of the above organisations and individuals is gratefully acknowledged.

In 2005-2006, the prediction method has been revised with financial support from Nordic Road Administrations mentioned above. The present report is replacing the earlier version of the report AV 1851/00.

The changes in the Nord2000 method which have taken place since 2001 have been summarized in the report AV 1307/06: “Changes in the Nord2000 method since year 2001”.

Validation of the model has been described in the report AV 1117/06: “Nord2000. Validation of the Propagation Model”.

Summary

A comprehensive model for propagation of sound in an atmosphere without significant refraction has been described in a companion report AV 1849/00: “Nord2000. Comprehensive Outdoor Sound Propagation Model. Part 1: Propagation in an Atmosphere without Significant Refraction”. In this model, which is based on geometrical ray theory combined with theory of diffraction, sound rays are assumed to follow straight lines.

In the present report it is described how the straight line model can be modified to include the effect of moderate atmospheric refraction by introducing circular sound rays in the propagation model. The modification is based on simple equations assuming that the sound speed varies linearly with the height above the ground in which case the rays will follow circular arcs.

Most often “uncomplicated” weather conditions are represented by an approximately logarithmic sound speed profile. Therefore, the crux has been to approximate such a non-linear sound speed profile by an equivalent linear profile. A principle has been elaborated for determination of the equivalent linear sound speed profile.

In case of strong downward refraction the model based on simple geometrical modification of rays has been extended to include the effect of additional rays from multiple reflections.

In case of strong upward refraction where no ray will reach the receiver in a shadow zone the model has been extended to include effects of shadow zones.

1. Introduction

The Nord2000 comprehensive model for propagation of sound in an atmosphere without significant refraction has been described in detail in [4]. In this model, which is based on geometrical ray theory combined with theory of diffraction, sound rays are assumed to follow straight lines.

In the present report it is described how the straight line model in [4] can be modified to include the effect of moderate atmospheric refraction by introducing curved sound rays in the propagation model. An efficient approach with respect to calculation time is to assume that the sound speed varies linearly with the height above the ground in which case the sound rays will be circular arcs as described by L'Espérance [2]. The circular arcs can be determined by fairly simple formulas.

An alternative to the chosen method could have been numerical ray tracing which can be used for non-linear sound speed profiles. However, such a method is considerably more time consuming than the chosen method and the general impression is that the method will not yield significantly better results in most cases, but on the contrary is somewhat unstable and produces erroneous results in special cases. Other possibilities could have been numerical calculation methods such as e.g. the PE method (Parabolic Equations) or FFP (Fast Field Program). However, these methods are extremely time-consuming and cannot be used as a basis of an engineering method.

The aim of the Nordic project has been to develop a propagation model with sufficient accuracy for "uncomplicated" weather conditions. These are weather conditions where the sound speed is either decreasing or increasing monotonically with the altitude without significant jumps in the sound speed gradient. Most often such "uncomplicated" weather can approximately be represented by sound speed profile with a logarithmic and a linear part called log-lin profiles. The crux when using the linear sound speed profile concept [2] has been how to approximate a non-linear sound speed profile by an equivalent linear profile. The method that has been elaborated for this purpose is not expected to be applicable in case of irregularly shaped sound speed profiles.

In case of strong downward refraction the model based on simple geometrical modification of rays has to be extended to include the effect of multiple reflections. Also in case of strong upwind where no ray will reach the receiver in a shadow zone the model has to be extended to include effects of shadow zones.

The elaboration of the comprehensive model has been carried out since 1996 and subtasks within the project have along the way been reported in a number of background reports. Contrary to the present report these reports contain a discussion of the solutions and comparison of prediction results with measurements or with results obtained by other prediction models. The background reports which are of relevance to the modifications for a refracting atmosphere are:

- [5] contains an overall description of the modifications that have been introduced in the straight line model to account for the effect of refraction.
- [6] describes the method elaborated for approximating a non-linear sound speed profile by an equivalent linear profile.
- [10] contains a discussion of the influence of a refracting atmosphere on screening and ground effect.
- [11] describes a method for including the effect of multiple reflections in case of strong downward refraction.
- [8] contains a discussion of the linear sound speed profile approach in [2].
- [9] contains comparisons between results obtained by the linear sound speed profile approach and results by FFP.
- [1] contains equations for calculating circular ray paths for a linear sound speed profile.

The model described in the present report may reflect changes that have taken place in the principles since the background reports have been published.

All 2-D features of the propagation model described in the present report and in [4] have been implemented in Matlab code which serves as a reference software.

Section 2 below contains the equations which are used to determine the circular rays and Section 3 describes the method for approximating a non-linear sound speed profile by an equivalent linear profile. Section 4 through 8 describe the modifications introduced in the models for determining the propagation effect of spherical divergence, air absorption, terrain and screens, scattering zones and reflections (corresponding to Section 2 through 6 in [4], respectively).

2. Basic Principle. Modification of Sound Rays

The effect of atmospheric refraction is taken into account in the comprehensive outdoor sound propagation model by replacing the straight rays in the model for a homogeneous atmosphere [4] by curved rays. In the model it is assumed that the sound speed profile varies linearly with the height above the ground surface as defined in Eq. (1), where c(0) is the sound speed at the ground, z is the height above the ground and $\Delta c/\Delta z$ is the sound speed gradient.

$$c(z) = c(0) + \frac{\Delta c}{\Delta z} z \tag{1}$$

Sound profiles will seldom be linear in practice. Therefore a principle has been elaborated for approximating a non-linear sound speed profile by an equivalent linear profile [6]. This principle is described in Section 3.

In the case where sound propagates over a flat finite impedance surface the modification of rays concerns the direct ray as well as the reflected ray. Figure 1 and Figure 2 show the modified rays in case of downward refraction ($\Delta c/\Delta z > 0$) and in case of upward refraction ($\Delta c/\Delta z < 0$), respectively.

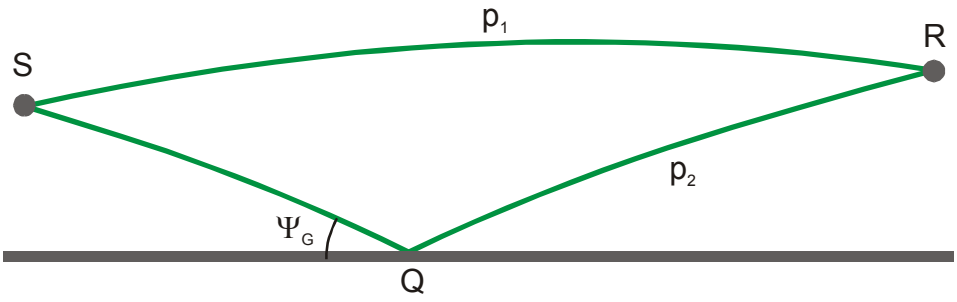

Figure 1
Sound propagation over flat terrain in case of downward refraction.

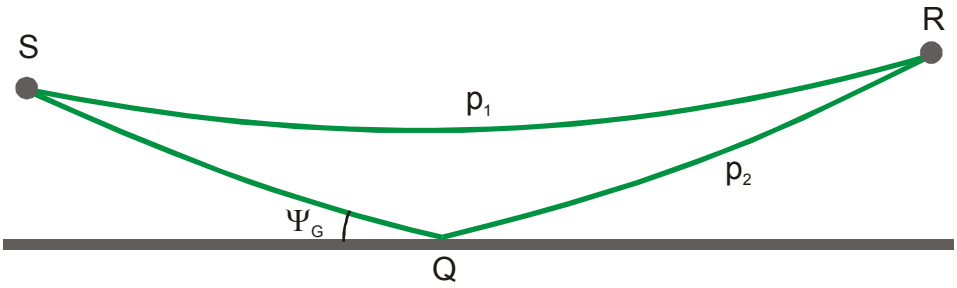

Figure 2
Sound propagation over flat terrain in case of upward refraction.

2.1 Modification of the Direct Ray

Basically the purpose of introducing circular rays is to modify the variables in the free-space Green's function shown in Eq. (2). The attenuation due to spherical divergence is expressed by the term $1/R_0$ in Eq. (2) where R_0 is the direct distance between the source and receiver. In the case of refraction this distance is replaced by the distance R measured along the curved ray as shown in Eq. (3). The phase is expressed by the term $\exp(jkR_0)$ in Eq. (2) where j is the complex unit and k is the wave number. In case of refraction this term is replaced by $\exp(j\omega\tau)$ where ω is the angular frequency ($\omega = 2\pi f$ where f is the frequency) and τ is the travel time along the curved ray.

$$p = \frac{e^{jkR_0}}{R_0} \tag{2}$$

$$p = \frac{e^{j\omega\tau}}{R} \tag{3}$$

In excess of R and τ the change in angle $\Delta\theta$ between the circular ray and the straight line ray has to be determined when the diffraction effect has to be predicted as described in Section 6.2. Figure 3 defines the parameters R, τ and $\Delta\theta$ when the sound is propagating between points L and U where L is the lower position and U is the upper position. L and U can be the source, receiver or edges of screens.

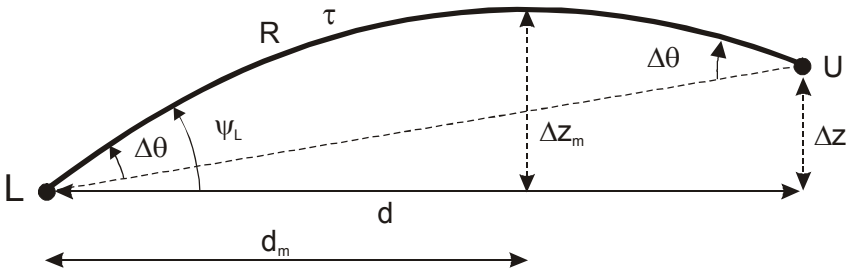

Figure 3
Definition of geometrical parameters for a circular direct ray.

In order to use the method described in [2] the sound speed profile in Eq. (1) has to be rewritten as shown in Eq. (4) where $c_0 = c(z_L)$ is the sound speed at the lowest point L, Δz is the difference in height between U and L and ξ is the relative sound speed gradient. ξ is defined by Eq. (5) where $\Delta c/\Delta z$ is the linear sound speed gradient.

$$c(z) = c_0\left(1 + \xi\left(z - z_L\right)\right) \tag{4}$$

$$\xi = \frac{\Delta c/\Delta z}{c_0} \tag{5}$$

Δz is in the following defined as the shown in Eq. (6) where z_L and z_U are the heights of point L and U above ground.

$$\Delta z = z_U - z_L \tag{6}$$

The first step towards the determination of R, τ and $\Delta\theta$ will be to calculate the angle ψ_L and horizontal distance d_m from L to the extremum of the circle which contains the circular arc as shown in Figure 3. ψ_L and d_m are calculated by Eqs. (7) and (8).

$$\tan\psi_L = \frac{\xi\, d}{2} + \frac{\Delta z\,(2 + \xi\,\Delta z)}{2d} \tag{7}$$

$$d_m = \frac{\tan\psi_L}{\xi} \tag{8}$$

If $\xi > 0$ and $d \le d_m$, R and τ are calculated by Eqs. (9) to (12).

$$R(\Delta z) = \frac{1}{\xi\cos(\psi_L)}\left(\arcsin\left((1 + \xi\,\Delta z)\cos(\psi_L)\right) - \frac{\pi}{2} + \psi_L\right) \tag{9}$$

$$\tau(\Delta z) = \frac{1}{2\,\xi\,c_0} \ln\left(\frac{f(0)}{f(\Delta z)}\right) \tag{10}$$

where

$$f(0) = \frac{1+\sin\psi_L}{1-\sin\psi_L} \tag{11}$$

and

$$f(\Delta z) = \frac{1+\sqrt{1-(1+\xi\Delta z)^2\cos^2\psi_L}}{1-\sqrt{1-(1+\xi\Delta z)^2\cos^2\psi_L}} \tag{12}$$

If $d > d_m$, R and τ are instead calculated by Eqs. (13) to (15) where Δz_m is the height of the ray at the extremum of the circle at the horizontal distance d_m. $R(\Delta z_m)$ and $R(\Delta z)$ are calculated by Eq. (9) and $\tau(\Delta z_m)$ and $\tau(\Delta z)$ by Eq. (10).

$$\Delta z_m = \frac{1}{\xi}\left(\frac{1}{\cos(\psi_L)} - 1\right) \tag{13}$$

$$R = 2\,R(\Delta z_m) - R(\Delta z) \tag{14}$$

$$\tau = 2\,\tau(\Delta z_m) - \tau(\Delta z) \tag{15}$$

Finally, the change in ray angle $\Delta\theta$ (see Figure 3) compared to the straight line ray can be determined by Eq. (16).

$$\Delta\theta = \psi_L - \arctan\left(\frac{\Delta z}{d}\right) \tag{16}$$

If $\xi < 0$, R, τ and $\Delta\theta$ are also determined by Eqs. (7) through (16) using the absolute value of ξ ($\xi = |\xi|$), but in this case the calculated value of $\Delta\theta$ is multiplied by –1 as shown in Eq. (17).

$$\Delta\theta(\xi < 0) = -\Delta\theta(\xi > 0) \tag{17}$$

The equations shown above will when Δz is approaching 0 give rise to numerical problems when being implemented in computer code. Therefore, when Δz becomes less than 0.01 a value of 0.01 should be used instead. Furthermore, the equations cannot be used

when ξ becomes 0 (homogeneous atmosphere). Therefore, when $|\xi| < 10^{-10}$, $\xi = 10^{-10}$ has to be used instead.

2.2 Modification of the Reflected Ray

The first step when calculating the modified parameters of the reflected ray will be to determine the reflection point. The geometrical parameters of the reflected ray are defined in Figure 4.

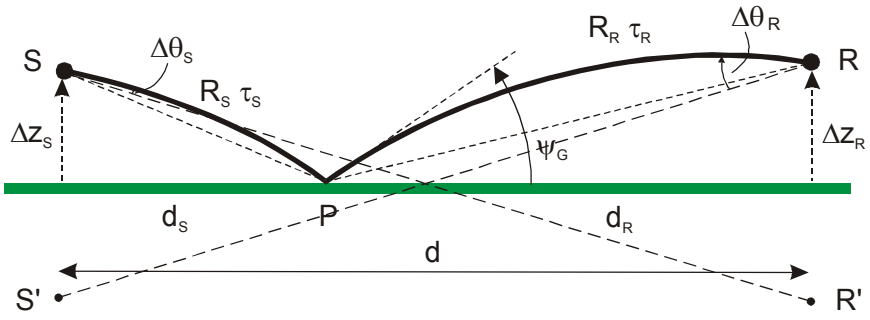

Figure 4
Definition of geometrical parameters for a circular reflected ray.

For the reflected ray the sound speed profile is again defined by Eqs. (4) to (5), but in this case $c_0 = c(0)$ is the sound speed at the ground and Δz is the height of S or R above the ground.

In downward refraction ($\xi > 0$) the reflection point is determined by solving Eq. (18) with respect to d_S where d is the horizontal propagation distance and d_S is the horizontal distance from the source to the reflection point P. b_S^2 and b_R^2 are given by Eqs. (19) and (20). A method for solving Eq. (18) can be found in [3].

$$2d_S^3 - 3dd_S^2 + (b_R^2 + b_S^2 + d^2)d_S - b_S^2 d = 0 \tag{18}$$

$$b_S^2 = \frac{z_S}{\xi}(2 + \xi z_S) \tag{19}$$

$$b_R^2 = \frac{z_R}{\xi}(2 + \xi z_R) \tag{20}$$

Eq. (18) may have up to three real solutions for large values of ξ. If the equation has more than one solution, the reflection point closest to the source is used when the source height is less than the receiver height while the reflection point closest to the receiver is used

when the source height is greater than the receiver height. This approach ensures that there are no discontinuities when the number of solutions in Eq. (18) switches between one and three. However, the approach will unavoidable have a discontinuity when source and receiver have the same height.

Before determining the reflection point in the upward refraction case ($\xi < 0$) it has to be investigated whether the receiver may be in the shadow zone. The receiver is in the shadow zone if Eq. (21) is fulfilled.

$$d > \sqrt{z_S\left(\frac{2}{|\xi|} - z_S\right)} + \sqrt{z_R\left(\frac{2}{|\xi|} - z_R\right)} \tag{21}$$

To avoid numerical problems in the calculations at the edge of the shadow zone it is recommended to fulfil the equation with a margin of 5% (multiply the right side of the equation by 0.95).

If the receiver is not in the shadow zone, the reflection point can again be found by solving Eq. (18). However, in this case there will only one real solution.

After having determined the reflection point the distance R, the travel time τ, and the grazing angle of the reflection ψ_G can be determined for the circular arcs before and after reflection point separately using the method described in Section 2.1. Subsequently the changes in ray angles $\Delta\theta_S$ and $\Delta\theta_R$ at the source and receiver relative to the homogeneous case can be determined by Eqs. (22) and (23).

$$\Delta\theta_S = \psi_G + \arctan\frac{z_S + z_R}{d} - 2\arctan\frac{z_S}{d_S} \tag{22}$$

$$\Delta\theta_R = \psi_G + \arctan\frac{z_S + z_R}{d} - 2\arctan\frac{z_R}{d_R} \tag{23}$$

When using the equations of Section 2.1 for the arc between the source and the reflection point the parameters to be used are $\Delta z = z_S$, $d = d_S$, $c_0 = c(0)$ and ξ based on this value of c_0. The calculated values are denoted R_S, τ_S, $\Delta\theta_S$ and ψ_G is equal to ψ_L.

For the arc between the receiver and the reflection point the parameters to be used are $\Delta z = z_R$, $d = d_R$, $c_0 = c(0)$ and ξ based on this value of c_0. The calculated values are denoted R_R, τ_R and $\Delta\theta_R$.

Finally the total path length along the reflected ray is given by $R = R_S + R_R$ and the travel time by $\tau = \tau_S + \tau_R$.

2.3 Differences between Direct and Reflected Rays

The travel times τ_1 and τ_2 of the direct and reflected rays calculated as described in Section are used to calculate the travel time difference $\Delta\tau=\tau_2-\tau_1$ which determines the difference in phase between the direct and reflected ray (see Eq. (38). As the phase differences are essential to sound interference effects it is there very important that the travel times are calculated with a high accuracy.

For very high sources (or receivers) the calculation of the travel time difference $\Delta\tau$ as described above has been found to fail upward refraction at the edge of a meteorological shadow zone.

To solve the problem a maximum travel time difference $\Delta\tau_0$ is calculated by (24) where h_S and h_R is the source and receiver heights, d and d_{SZ} are the source-receiver distance and distance from source to shadow zone measured along the ground and C is the sound speed at the ground.

$$\Delta\tau_0 = \frac{\left(1-\left(\frac{d}{d_{sz}}\right)^2\right)\left(\sqrt{d^2+(h_S+h_R)^2}-\sqrt{d^2+(h_S-h_R)^2}\right)}{C} \tag{24}$$

If $\Delta\tau$ is greater than $\Delta\tau_0$, the latter is used instead. This ensures that $\Delta\tau$ will be zero at the edge of the shadow zone.

3. Equivalent Sound Speed Profile

The aim of the Nordic project has been to develop a propagation model with sufficient accuracy for “uncomplicated” weather conditions. These are weather conditions where the sound speed is either decreasing or increasing monotonically with the altitude without significant jumps in the sound speed gradient. Most often such “uncomplicated” weather can approximately be represented by sound speed profile with a logarithmic and a linear part called log-lin profiles. The crucial point when using the linear sound speed profile concept described in Section 2 has been how to approximate a non-linear sound speed profile by an equivalent linear profile.

It is assumed that the method developed in [6] for determining the equivalent linear sound speed profile will be applicable when the effective sound speed profile approximately can be described by a simple combination of a logarithmic and a linear relationship as shown in Eq. (25). The effective sound speed is the combined effect of the sound speed in air and the wind speed in the direction of propagation. In Eq. (25) z is the height above the ground surface, z_0 is the roughness length and A, B and C are constants.

$$c(z) = A \ln\left(\frac{z}{z_0} + 1\right) + B\,z + C \tag{25}$$

***Note**: The elaborated method will not be applicable in case of irregularly shaped sound speed profiles, but it is difficult to state the magnitude of deviations from Eq. (25) that can be allowed.*

When calculating the yearly average of the weather as described in [13] for the Nordic countries and in [12] for the European Union the calculation are based on a number of meteo-classes and each meteo-class is defined by A, B, and C.

If the logarithmic part of the profile only is determined by the wind speed component u in the direction of propagation is given at height z_u, A can be determined by Eq. (26).

$$A = \frac{u(z_u)}{\ln\left(\frac{z_u}{z_0} + 1\right)} \tag{26}$$

If the linear part of the profile only is determined by the temperature and is assumed to increase linearly with the height (dt/dz is constant), the sound speed can approximately be assumed to be a linear function of the height with a value of B given by Eq. (27).

$$B = \frac{dt}{dz}\frac{10.025}{\sqrt{t + 273.15}} \tag{27}$$

The parameters $\Delta c/\Delta z$ and c(0) which define the equivalent linear sound speed profile in Eq. (1) is determined by Eqs. (28) to (30). The gradient $\Delta c/\Delta z$ is determined as the average gradient between the heights h_S and h_R and the equivalent linear profile is passing through the average sound speed $\bar{c}$ at the average height between h_S and h_R.

$$\frac{\Delta c}{\Delta z} = \frac{c(h_R) - c(h_S)}{h_R - h_S} \tag{28}$$

$$\bar{c} = \frac{1}{h_R - h_S}\int_{h_S}^{h_R} c(z)\,dz \tag{29}$$

$$c(0) = \bar{c} - \frac{\Delta c}{\Delta z}\frac{h_S + h_R}{2} \tag{30}$$

If h_S becomes equal to h_R, $\Delta c/\Delta z$ and $\bar{c}$ and in Eqs. (28) and (29) are the gradient dc/dz and sound speed c at h_S. **?**

To avoid extreme values of $\Delta c/\Delta z$ in case of low source and receiver a minimum height h_{min} has been introduced in the calculation of the equivalent linear sound speed profile. h_{min} is 5 times the roughness length z_0 defined in Eq. (25). If h_S and h_R used in Eqs. (28) to (30) are below h_{min}, h_{min} is used instead.

When calculating ground effect of hard surfaces (flow resistivity larger than 10,000,000 Nsm^{-4}), diffraction effects, and Fresnel zones, the equivalent linear sound speed profile is assumed to be independent of the frequency and determined by $\Delta c/\Delta z$ and c(0) given above.

***Note**: At present only the Delany and Bazley impedance model is used in the Nord2000 model and the frequency dependent sound speed profile linearization principle described in the following is closely related to this impedance model. If other impedance models are applied, a preliminary investigation shows that a frequency independent linearization should be preferred until this has been investigated more closely.*

In case of ground effects of non-hard surfaces the equivalent linear sound speed profile will depend on the frequency. Above a certain frequency f_H the equivalent linear sound speed profile is determined in the same way as described above for diffraction effects, but below a frequency f_L $\Delta c/\Delta z = 0$ and $c(0) = \bar{c}$ corresponding to a homogeneous atmosphere. Between f_L and f_H transition values $\Delta c'/\Delta z$ and $c'(0)$ given by Eqs. (31) and (32) are used.

$$\frac{\Delta c'}{\Delta z} = \frac{\log f - \log f_L}{\log f_H - \log f_L} \frac{\Delta c}{\Delta z} \tag{31}$$

$$c'(0) = \bar{c} - \frac{\Delta c'}{\Delta z} \frac{h_S + h_R}{2} \tag{32}$$

The calculation of f_L and f_H is based on the frequencies f_π and $f_{2\pi}$ which correspond to the first dip and the subsequent peak in the ground effect spectrum for propagation in a homogeneous atmosphere without refraction. f_π and $f_{2\pi}$ are the frequencies where the phase difference between the direct and the reflected ray is π and 2π, respectively. The phase difference $\Delta\alpha$ as a function of the frequency f can approximately be determined by Eq. (33), where c(0) is defined above, ΔR is the difference in path length of the reflected and direct straight line ray and R_p is the plane wave reflection coefficient. When calculating $\Delta\alpha$ the source and receiver heights h_S and h_R has to be modified when small while the propagation distance d has to be modified when large. If $h_S < 0.5$ m or $h_R < 0.5$ m, a value of 0.5 m is used, and if $d > 400$ m, a value of 400 m is used.

$$\Delta\alpha \approx \frac{2\pi f}{c(0)} \Delta R + \arg\left(R_p\right) \tag{33}$$

For accurate determination of $\Delta\alpha$, R_p should in Eq. (33) be replaced by the spherical wave reflection coefficient Q. However, as f_π and $f_{2\pi}$ have to be determined by iteration, the calculation of Q is much too slow for this purpose and Eq. (33) has proven sufficiently accurate for determining the first dip for other purposes as previously described in [4].

***Note**: An adequate procedure for determining f_π and $f_{2\pi}$ can be to calculate $\Delta\alpha$ at the one-third octave band centre frequencies from 25 Hz to 10 kHz and determine the exact frequency by logarithmic interpolation with the frequency between the one-third band results on each side of the desired value of $\Delta\alpha$. Below 25 Hz logarithmic extrapolation with the frequency is used and above 10 kHz linear extrapolation with the frequency is used.*

f_L and f_H are determined by Eqs. (34) and (35).

$$f_L = f_\pi \tag{34}$$

$$f_H = \sqrt{f_L \, f_{2\pi}} \tag{35}$$

At high downwind speeds it has been found in [6] that f_L should be reduced slightly compared to the prediction by Eq. (34). A modified value of f_L determined by Eq. (37) for values of Δc_{10} larger than 1 m/s has been found to produce somewhat better results around the first dip. Δc_{10} is the difference in effective sound speed c between z =10 m and z = 0 m determined by Eq. (25). If Δc_{10} exceeds 5 m/s $f_L = 0.7\, f_\pi$ is used. **?**

$$f_L = f_\pi \frac{43 - 3\Delta c_{10}}{40} \tag{36}$$

If f_L and f_H are too close defined by $f_L > 0.8\, f_H$, the frequency f_H is modified to $f_H = f_L/0.8$.

4. Spherical Divergence

In principle, the propagation effect of spherical divergence of the sound energy ΔL_d shall calculated by Eq. (37) (from Eq. (2) in [4]) where R in the distance between source and receiver measured along the free-field ray.

$$\Delta L_d = -10 \log \left(4 \pi R^2\right) \tag{37}$$

However, in the practical implementation of Nord2000 it is recommended to use another approach where ΔL_d is defined as the effect of spherical divergence for a homogeneous atmosphere and the terrain and screen effect ΔL_t is defined as the sound pressure level including weather effects relative to the free field level a for a homogeneous atmosphere.

5. Air Absorption

In [4] the effect of air absorption is determined for a homogeneous atmosphere based on air temperature and relative humidity. For an inhomogeneous refracting atmosphere the calculation shall in principle be based on the distance between source and receiver along the free-field ray and take into account that temperature and relative humidity will vary along the propagation path.. However, spatial information on relative humidity will seldom be available and a value obtained in a single or a few points has therefore to be used as representative of the entire propagation path. Also in the case of temperature it has not been found that the accuracy will increase sufficiently to justify such an advanced approach.

Instead a simple approach has been chosen where the representative temperature is defined as the temperature at the average value of the local source and receiver height and the distance used in the calculation is the direct source receiver distance.

6. Terrain and Screen Effects

The comprehensive model for terrain and screen effects for propagation through a homogeneous atmosphere (straight line propagation) described in [4] can be modified to include curved rays according to the principles outlined in the previous sections of the present report as long as the number of rays in the base models remains unchanged. This is fulfilled when the weather conditions are not causing multiple ground reflections (strong downward refraction) or shadow zones (strong upward refraction). In these cases the refraction problem can no longer be solved by simple geometrical modification of rays, but calls for a real extension of the model.

In the comprehensive model described in [4] a prediction for a complex terrain is carried by one of three propagation models named “flat terrain”, “valley-shaped terrain” or “hill-shaped terrain” or by a combination of the three models.

The three propagation models are according to [4] founded on three base models:

1) Flat terrain

2) One screen with a flat reflecting surface before and after the screen

3) Two screens with a flat reflecting surface before, after and between the screens

Therefore, prediction for any complex terrain is always the result of predictions by the three base models combined in a suitable manner by the Fresnel-zone interpolation principle and the model transition principles of [4]. This implies that, when the problem of using curved rays has been solved for each of these basic models, and the Fresnel-zone interpolation principle and model transition principles have been modified to deal with

curved rays, the problem has been solved for the entire comprehensive terrain and screen effect model.

In case of strong downward refraction additional rays will turn up due to multiple reflections. The contribution from such additional rays in excess of the rays already included in the modified ray model is calculated as described in Section 6.13 and is added incoherently to the predicted result of the modified comprehensive model described in the following. The method for including the contribution from multiple reflections is very approximate, and the accuracy of the overall model will in general decrease if there is a significant contribution from multiple reflections.

6.1 Flat Terrain

In the case of flat terrain the method for modifying sound rays described in Section 2 can be used directly as long as the receiver is not in the shadow zone in case of upward refraction ($\Delta c/\Delta z < 0$).

The propagation effect of flat terrain ΔL is calculated by Eq. (38) (modification of Eq. (11) in [4]) where R_1 and R_2 are the length of the direct and the reflected ray, τ_1 and τ_2 are the corresponding travel times, ω is the angular frequency and ψ_G is the ground reflection angle calculated as described in Section 2.

$$\Delta L = 20 \log \left| 1 + \frac{R_1}{R_2} Q(\psi_G, \tau_2)\, e^{j\omega(\tau_2 - \tau_1)} \right| \tag{38}$$

In case of strong upward refraction no ray reaches the receiver in the model for flat terrain, resulting in an acoustical shadow zone as shown in Figure 5. If the receiver is in the shadow zone, the modified ray model cannot be used for the calculation of the ground effect. Eq. (21) in Section 2 can be used to determine whether the receiver is in a shadow zone or not.

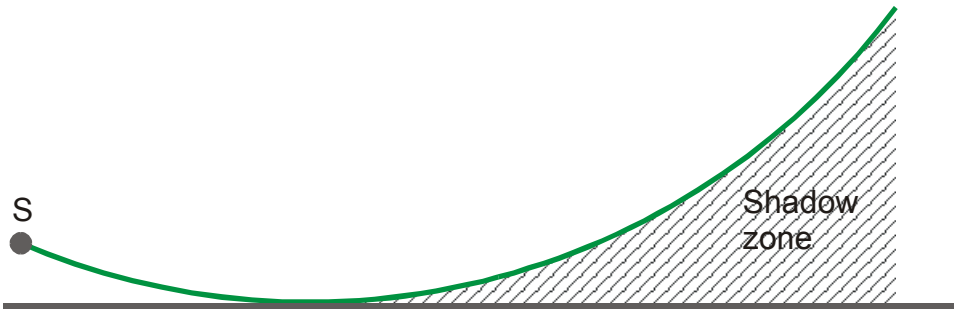

Figure 5
Acoustical shadow zone.

The difficult problem of a meteorologically generated shadow zone in the case of propagation over flat terrain has been considered analogous to the problem of predicting sound levels in the shadow zone behind a diffracting wedge in case of a non-refracting atmosphere as discussed in [5]. The task has been to elaborate a method based on this idea which fits into the structure of the comprehensive model and which does not introduce a discontinuity at the edge of the shadow zone.

At the edge of the shadow zone the direct and reflected ray become identical and graze the ground ($\psi_G = 0$). Therefore the ground effect ΔL can be expressed by Eq. (39) as $\tau_1 = \tau_2$. Q is determined using the curved path length $R = R_1$ of the direct ray and the reflection angle $\psi_G = 0$.

$$\Delta L = 20 \log \left| 1 + Q(\psi_G = 0, \tau_2 = \tau_1) \right| \tag{39}$$

To avoid discontinuities at the edge of the shadow zone the ground effect in the shadow zone is divided into a reflection effect contribution ΔL_G and a shadow zone shielding effect contribution ΔL_{SZ} as shown in Eq. (40).

$$\Delta L = \Delta L_G + \Delta L_{SZ} \tag{40}$$

ΔL_G is calculated based on Eq. (39) where Q is calculated on the basis of $\psi_G = 0$ and the path length R for the ray from the source to the receiver disregarding the ground as shown in Figure 6. Although R will increase the more the receiver moves into the shadow zone, the effect on ΔL_G will be almost negligible.

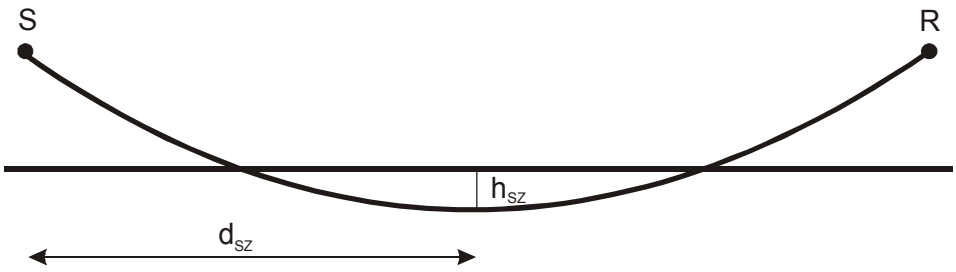

Figure 6
Ray used to calculate the reflection effect contribution in the shadow zone.

The horizontal distance d_{SZ} from the source to the reflection point when the receiver is at the edge of the shadow zone can approximately be determined by Eq. (41).

$$d_{SZ} = \frac{\sqrt{h_S}}{\sqrt{h_S} + \sqrt{h_R}} d \tag{41}$$

When the receiver is in the shadow zone, the vertical distance h_{SZ} between the ground surface and the ray from the source S to the receiver R at the horizontal distance d_{SZ} from the source shown in Figure 6 is used to define an equivalent wedge. The determination of h_{SZ} is described in Appendix A. The source S and receiver R is placed on the wedge faces as shown in Figure 7 with a distance between S and R of d. The top of the wedge is placed h_{SZ} above the line from the S to R at the distance d_{SZ} from S.

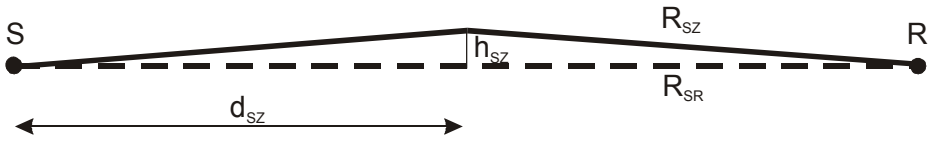

Figure 7
Equivalent wedge used to calculate the shielding effect contribution in the shadow zone.

The shadow zone shielding effect ΔL_{SZ} is determined using the diffraction solution for a wedge described in Appendix H in [4], but assuming that the wedge faces are totally absorbing ($Q_n = 0$ for all values of $n > 1$). ΔL_{SZ} is calculated by Eq. (42). R_{SR} is the direct distance from the source to the receiver and R_{SZ} is the distance over the top of the wedge. D_{SZ} is the diffraction coefficient calculated for the equivalent wedge (the wedge effect $\Delta L = 20 \log (|D_{SZ}|/R_{SZ})$). The constant 2 ensures that ΔL_{SZ} is 0 for a 180° wedge where D_{SZ} becomes 0.5.

$$\Delta L_{SZ} = 20 \log \left(2 \left| D_{SZ} \right| \frac{R_{SR}}{R_{SZ}} \right) \tag{42}$$

The flat terrain model is used in the following sections of [4]: Section 4.4.1.1 (flat terrain, homogeneous surface), Section 4.4.1.2 (flat terrain, varying surface properties) and Section 4.4.2 (valley-shaped terrain, concave and transition segments).

In the case of flat terrain with varying surface properties the refraction-modified model described above is used for each type of surface. The calculated results are then combined according to the Fresnel-zone model as described in [4]. The Fresnel zones used to calculate the Fresnel-zone weights are modified to include refraction as described in Section 6.6. In the calculation of the special weights in [4] the grazing angle ψ_G is replaced by the

refraction-modified value. In the calculation of the phase angle $\Delta\alpha$, $k(R_2-R_1)$ is replaced by $\omega(\tau_2-\tau_1)$ and $\Re_p$ is calculated on the basis of the modified grazing angle.

6.2 Wedge-Shaped Terrain and Screen

In case of a homogeneous atmosphere the calculation of the propagation effect of a finite impedance wedge is described in Appendix H of [4]. The calculation is based on the wedge angle β, the diffraction angles θ_S and θ_R and the distances R_S and R_R as shown in Figure 8.

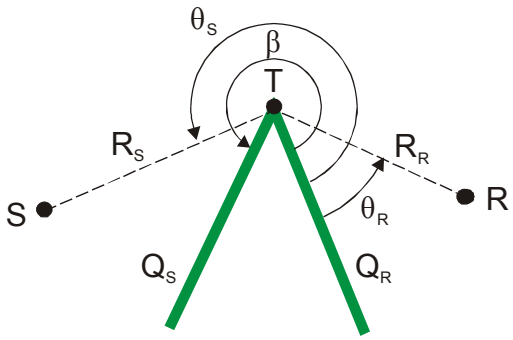

Figure 8
Definition of parameters for calculation of the propagation effect of a wedge-shaped screen with finite surface impedance in case of a homogeneous atmosphere.

In case of refraction the calculation is instead based on the modified diffraction angles θ_S and θ_R and the travel times τ_S and τ_R and the distances R_S and R_R measured along the circular arcs determined as described in Section 2. The modification of the method is mainly based on replacement of the distance R by the travel time τ and the replacement of the wave number k by the angular frequency ω. The modified method is described in detail in Appendix C.

The wedge-shaped terrain and screen model is used in Section 4.4.2 of [4] (valley-shaped terrain, convex and transition segments) and in Section 4.4.3.1 (diffraction of a finite impedance wedge).

6.3 Terrain with a Single Screen

For moderate downward and upward refraction the model for a single screen consists of 4 rays as shown in Figure 9 and Figure 10 in the same way as in the model for non-refracting atmosphere.

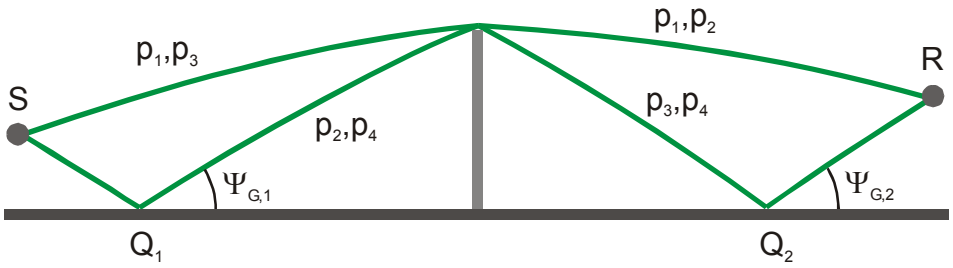

Figure 9
Ray model for a single screen and downward refraction.

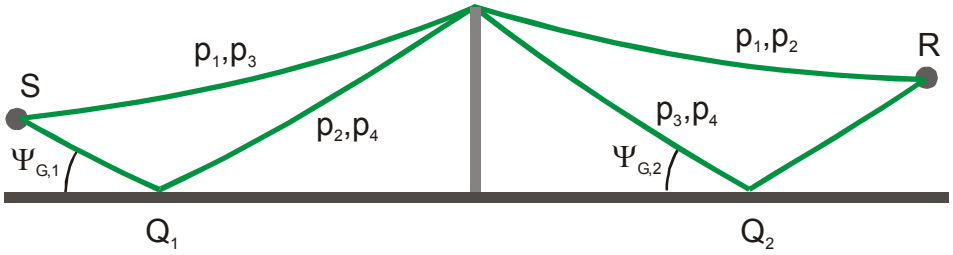

Figure 10
Ray model for a single screen and upward refraction.

In the screen model the modification of parameters concern the travel time τ and distance R along the circular rays as well as the ground reflection angles. Before the screen the rays are determined using the method for flat terrain, but with the receiver replaced by the screen top. After the screen the rays are determined with the source replaced by the screen top. In addition to that modified diffraction angles are determined on the basis of the modified rays before and after the screen.

As in the case of a homogeneous atmosphere the sound pressure level is calculated according to Eq. (43). p_1 to p_4 is calculated by the wedge model described in Section 6.2 based on the modified diffraction angles θ, travel times τ and distances R and p_0 is the sound pressure corresponding to the free-field circular ray (see Section 4). The spherical wave reflection coefficients Q_1 and Q_2 are based on the modified grazing angles ψ_G and distances R. The Fresnel-zone weight is modified as described in Section 6.6.

$$\Delta L = 20 \log \left| \frac{p_{1,s}}{p_0} \prod_{i=1}^{N_1} \prod_{j=1}^{N_2} \left(1 + \frac{p_{2,i,j}}{p_1} Q_{1i} + \frac{p_{3,i,j}}{p_1} Q_{2j} + \frac{p_{4,i,j}}{p_1} Q_{1i} Q_{2j} \right)^{w_{1i} w_{2j}} \right| \qquad (43)$$

However, the curvature of the direct ray used to calculate p_1 is not determined in the same way in the screen part of the propagation effect which is the term p_1/p_0 before the product signs and in the ground effect part which is the term after the product signs. This is indicated in Eq. (43) by the subscript s added to p_1 in the screen part.

In the ground effect part of Eq. (43) the equivalent linear sound speed profile defined by $\Delta c/\Delta z$ and $c(0)$ is determined on the basis of heights of the source and screen top above the reflecting surface before the screen and on the basis of heights of the receiver and screen top after the screen. Therefore, $\Delta c/\Delta z$ and $c(0)$ will normally differ before and after the screen.

If the same principle had been used for the screen part of the propagation effect, the refraction effect during downwind propagation would in the case of a thin screen as shown in Figure 9 and Figure 10 be less than in the case of a wedge as shown in Figure 11 where the height of the screen top above the reflecting surface is 0. Unfortunately, studies of propagation over screens during downwind conditions indicate that the opposite is the case due to screen-induced wind speed gradients.

Therefore, it has been chosen to calculate the equivalent linear sound speed profile on the source side of the screen on the basis of the local source height h_S and a modified screen height h'_{scr}. On the receiver side of the screen the local receiver height h_R and the height h'_{scr} is used. According to this principle the refraction effect will at least be the same for the thin and wedge-shaped screen case. Again, $\Delta c/\Delta z$ and $c(0)$ will normally differ before and after the screen.

The modified screen height is determined by Eq. (44) if $R' > 75$. R' is determined by Eq. (45) where R_{SR} is the distance from source to receiver, R_{ST} is the distance from source to screen top, and R_{RT} is the distance from receiver to screen top. If $R' < 75$, $h'_{scr} = 0$.

$$h'_{scr} = 4\frac{R' - 75}{135} \tag{44}$$

$$R' = R_{SR} + \min(R_{ST}, R_{RT}) \tag{45}$$

The implication of the principle described above for linearization for the screen part of the propagation effect is that the gradient of the equivalent linear sound speed profile will decrease with increasing propagation distance contrary to the principle used for the ground effects.

***Note**: In connection with the elaboration of the method described above it has not been possible to study the effect of the screen on the airflow over the screen properly. It is known that the effect of screen-induced wind speed gradients may affect the performance of a screen seriously especially when the source and the receiver are close to the screen [7]. The method outlined above for the screen part of the propagation effect has roughly been adjusted to account for screen-induced wind speed gradients. However, it must strongly be recommended in connection with future developments to study this more closely.*

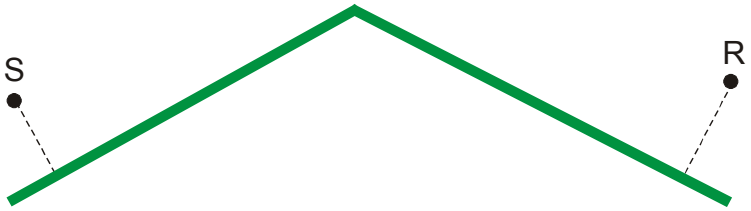

Figure 11
Propagation over a wedge shape.

In the case of strong upward refraction the ray from the source to the top of the screen or from the top of the screen to the receiver may be blocked by the ground, resulting in acoustical shadow zones. The problem of shadow zones in the case of a screen has been solved analogously to flat terrain. If a shadow zone occurs before, after, or on both sides of the screen, the ground effect term p/p_1 of Eq. (43) for the i'th segment on the source side and j'th segment on the receiver side shown in Eq. (46) is replaced by Eqs. (47) to (49) respectively. $\Delta L_{SZ,1}$ is the excess shielding effect on the source side of the screen and is calculated using the same procedure as for flat terrain, but with the receiver placed on the top of the screen. In the same way $\Delta L_{SZ,2}$ is the excess shielding effect on the receiver side of the screen, but with the source placed on the top of the screen.

$$\frac{p}{p_1} = 1 + \frac{p_{2,i,j}}{p_1} Q_{1i} + \frac{p_{3,i,j}}{p_1} Q_{2j} + \frac{p_{4,i,j}}{p_1} Q_{1i} Q_{2j} \tag{46}$$

$$\frac{p}{p_1} = \left(1 + \frac{p_{3,i,j}}{p_1} Q_{2j}\right)\left(1 + Q_{1i}\right) 10^{\Delta L_{SZ,1i}/20} \tag{47}$$

$$\frac{p}{p_1} = \left(1 + \frac{p_{2,i,j}}{p_1} Q_{1i}\right)\left(1 + Q_{2j}\right) 10^{\Delta L_{SZ,2j}/20} \tag{48}$$

$$\frac{p}{p_1} = \left(1 + Q_{1i}\right)\left(1 + Q_{2j}\right) 10^{\Delta L_{SZ,1}/20} 10^{\Delta L_{SZ,2}/20} \tag{49}$$

The modifications in this section concern Section 4.4.3.4 in [4].

6.4 Terrain with Double Screens

For moderate downward and upward refraction the model for double screens includes 8 rays as in the model for a non-refracting atmosphere. The modifications in the double screen model concern the travel time τ and distance R between source, screen tops and receiver, the ground reflection angles before, after and between the screen and the diffraction angles determined in the same way as in the single screen case. Before the first screen

(based on an equivalent linear sound speed profile defined by $\Delta c_1/\Delta z$ and $c_1(0)$) and after the second screen (based on an equivalent linear sound speed profile defined by $\Delta c_3/\Delta z$ and $c_3(0)$) the procedure is the same as described in Section 6.3 for a single screen and the modified screen height h'_{scr} given by Eq. (44) is in both cases used to determine the ray curvature.

Between the screens the ray curvature for the screen part of the propagation effect is determined with a "source" and "receiver" height both equal to the modified screen height h'_{scr} leading to an equivalent linear sound speed profile defined by $\Delta c_2/\Delta z$ and $c_2(0)$. For the ground part the equivalent linear sound speed profile is again determined differently using the heights above the reflecting surface.

Depending on whether shadow zones occur before, between and/or after the screens, Eqs. (47) to (49) is replaced by seven equations using the same principles and involving the excess shielding effects $\Delta L_{SZ,1}$, $\Delta L_{SZ,2}$ and $\Delta L_{SZ,3}$ before, between and after the screens.

The modifications in this section concern Sections 4.4.3.2 and 4.4.3.5 in [4].

6.5 Two-Edge Screens

The approach for the section of the screen between the two edges when determining the circular rays for a two edge screen is identical to the approach described above for double screens concerning the screen effect part of the propagation effect.

This concerns Sections 4.4.3.3 and 4.4.3.4 in [4].

6.6 Fresnel Zone

As mentioned in the introduction of Section 6 the Fresnel-zone interpolation principle has to be modified to deal with curved rays. This is done by bending the Fresnel-zone ellipsoid so that its axis of rotation follows the circular ray. Practically, this is done by transforming the curved ray case into a straight line ray case leading to modified source and receiver positions S' and R'. The straight line case is defined by the grazing angle ψ_G and the distances R_S and R_R determined for the curved ray. This is shown in Figure 12 where the size of the Fresnel zone is calculated using the algorithms for straight line propagation, but for the modified image source position S" and the modified receiver position R'.

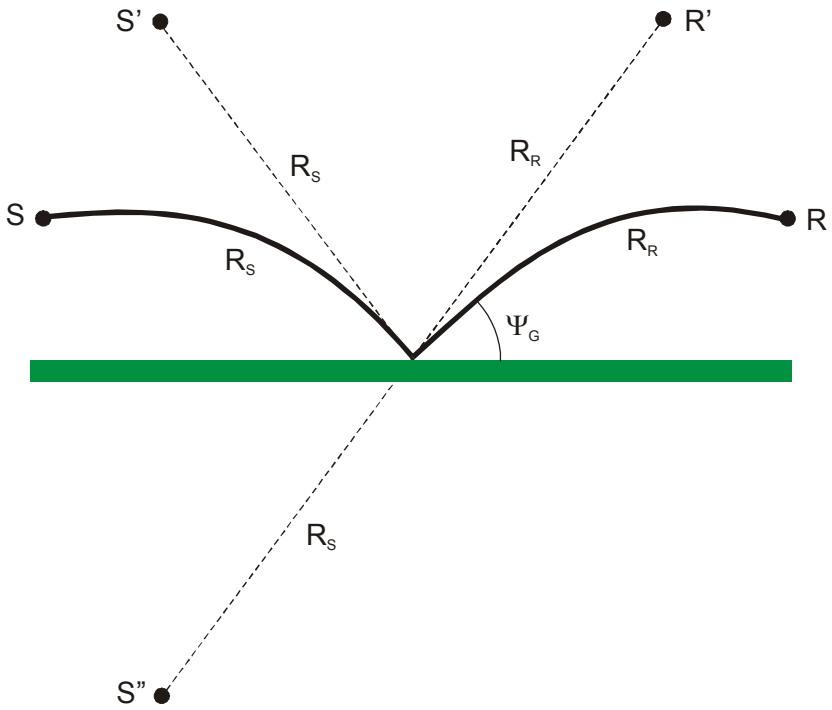

Figure 12
Determination of the Fresnel zone in case of curved rays.

The modified horizontal propagation distance d' and source and receiver height is determined by Eqs. (50) to (52).

$$d' = \left(R_S + R_R\right)\ \cos\psi_G \tag{50}$$

$$h_S^{'} = R_S\ \sin\psi_G \tag{51}$$

$$h_R^{'} = R_R\ \sin\psi_G \tag{52}$$

The modifications in this section concern Sections 4.2 in [4].

6.7 Transition between Propagation Models

The transition between the models for flat terrain and non-flat terrain which in the first place is quantified by the parameter r_f depends in the non-refraction case on the change in ΔR_2 determined on the basis of the average deviation of the terrain Δh from the equivalent flat terrain (as described in [4]). The logical approach would have been to determine ΔR_2 on the basis of curved rays in the refraction case, but it is not expected that there will be an increase in accuracy to justify this more difficult approach. It has therefore been decided to use the same method as in non-refraction case. However, for valley-shaped ter-

rain the modified transition parameter r_{flat} shall based on the sum of refraction-modified Fresnel-zone weights $w_{con,i}$.

The search for the most efficient edges in the primary and secondary screens is done assuming a homogeneous atmosphere (straight line rays). Therefore, the method for determining the edges is the same as described in [4]. This represents a modification of the original method where curved rays were used when selecting the edges. The reason for modification is that discontinuities have been observed when changing the magnitude of refraction due to a shift in selected edges with increasing or decreasing ray refraction. In some cases the noise level suddenly decreased with increasing downwind speed which was found to an undesirable behaviour. The proposed method for selection the edges might occasionally lead to a slight underestimation of the attenuation, but this has been considered preferable to the discontinuities.

In the refraction case, the transition terms r_λ and r_{Fz} which are based on the height of the screen are unchanged whereas the term $r_{\Delta\ell}$ based on the path length difference $\Delta\ell$ is modified to take the curved rays into account.

The determination of $\Delta\ell$ for a screen edge is based on the modified diffraction angles θ_S and θ_R and propagation distances R_S and R_R used to calculate the screen effect as mentioned in Section 6.2. If $\theta_S - \theta_R < \pi$, transition will take place, and the path length difference $\Delta\ell$ used to determine the transition parameter $r_{\Delta\ell}$ is calculated by Eq. (53). Same principle is used for the secondary screen or secondary edges, but in this case the source and/or receiver is replaced by a screen edge.

$$\Delta\ell = \sqrt{R_S^2 + R_R^2 - 2R_S R_R \cos(\theta_S - \theta_R)} - R_S - R_R \tag{53}$$

In the non-refraction case the transition parameters r_w or r_{w12} used to obtain a transition between the one and two screen case or between the one and two edge case, respectively, is based on the distance d_{12} between the most important edges of the two screens or between the two edges of a double edge screen. As the transition principle only will be of relevance when the distance d_{12} between the two involved edges is small the same principle is used in the refraction case disregarding that the rays should be curved.

The modifications in this section concern Sections 4.4.4 in [4].

6.8 Coefficients of Coherence

The coherence coefficient F_f is modified by replacing $k(R_2 - R_1)$ by $\omega(\tau_2 - \tau_1)$.

The coherence coefficient $F_{\Delta\tau}$ is already based on f and τ and does not have to be modified.

In the calculation of the coherence coefficients F_c k is determined on the basis of the average sound speed $\bar{c}$ determined by Eq. (29), c_0 is defined to be $\bar{c}$ and T_0 to be the temperature at the average of the local source and receiver height. The transversal separation ρ and the horizontal distance d is calculated in the same way as described in [4] for a homogeneous atmosphere.

The coherence coefficient F_r is modified by using the refraction-modified value ψ_G and defining $k = 2\pi f/c_G$ where c_G is the sound speed at the ground (z = 0) determined by Eq. (25).

The modifications in this section concern Sections 4.5.3 in [4].

6.9 Finite Screens

Finite screens are in the comprehensive model taken into account by applying the solution of an infinite screen, but adding the contribution from sound diffracted around the vertical edges of the screen [4]. This is done practically by adding an extra propagation path from the source via the vertical edge of the screen to the receiver.

As a path around the end of the screen is a broken line, the sound speed gradient may vary along the path in case of refraction caused by wind. This is solved by calculating a weighted average of sound speed profile along the path by the same method as introduced for a reflected ray path (described in Section 8). The weighted average is then used when calculating the propagation effect of the diffracted path.

The modifications in this section concern Sections 4.6 in [4].

6.10 Irregularly Shaped Screens

In [4] the height of an irregularly shaped screen is determined as the average height of the screen within the size of a Fresnel zone horizontally on each side of the propagation path. In case of refraction the propagation distance from source to receiver will increase somewhat leading to a minor increase in the size of the Fresnel zone. However, considering the fact that this is a very approximate approach, it has not been not been meaningful to modify the approach.

The modifications in this section concern Sections 4.7 in [4].

6.11 Special Screens

In [4] the attenuation of specially designed screens is taken into account by replacing the screen by a thin screen in the calculations and adding the extra attenuation of the special screen in excess of the attenuation by the thin screen in tabular form. The table is a four-parameter table using the thin screen parameters R_S, R_R, θ_S and θ_R as input parameters. In

case of refraction the same table is used with the refraction-modified values of the same parameters.

The modifications in this section concern Section 4.8 in [4].

6.12 Atmospheric Turbulence

In case of refraction the method described in Sections 4.9 of [4] for including the contribution from sound energy scattered from atmospheric turbulence into the shadow zone of a screen is used with a simple modification.

The effective height of the screen h_e is determined relative to a line between a modified source and receiver. The modified source and receiver positions can be defined by Figure 8 on the basis of the refraction-modified diffraction angles θ_S and θ_R and distances R_S and R_R.

In case of two screens or two edge screens the height of the edges are also determined relative to the refraction modified source-receiver line. The modified source position is determined on the basis of θ_S and R_S at the edge closest to the source and the modified receiver position is determined on the basis of θ_R and R_R for the edge closest to the receiver.

In a shadow zone generated by upward refraction over flat terrain the method can also be used by assuming $h_e = h_{sz}$, $R_1 = d_{sz}$ and $R_2 = d - R_1$. h_{sz} and d_{sz} are defined in Section 6.1.

6.13 Multiple Reflections

The objective of the present work has been to develop a sound propagation model applicable for a moderately refracting atmosphere. A moderately refracting atmosphere is defined indirectly as atmospheric conditions where the effect of additional rays during downward refraction is not dominating the overall propagation effect or where the receiver is not deep inside a shadow zone. However, both effects may occur at fairly small distances in case of strong refraction and it has been found expedient – in an approximate manner – to extend the model to cover such cases.

An approximate model for shadow zones has been presented in Sections 6.1 to 6.3.

In the present section a simple method [11] for including the propagation effect of additional rays will be described. The contribution from rays in excess of the rays already included in the models described previously is calculated and added incoherently to obtain the overall effect.

The method in [11] has been developed for at logarithmic sound speed profile as shown in Eq. (54) and for propagation over flat terrain.

$$c(z) = A \ln\left(\frac{z}{z_0} + 1\right) + C \tag{54}$$

The first step is to determine the approximate number of rays N (decimal number) by Eq. (55) where d is the horizontal propagation distance, h_{max} is the maximum value of the source height h_S and the receiver height h_R and A and C are the constants in Eq. (54).

$$N = \frac{4d}{h_{\max}}\sqrt{\frac{A}{2\pi C}} \tag{55}$$

For a value of N smaller than 4 there will be no contribution from additional ray whereas the contribution will be calculated as described in the following for larger values.

The number N is divided in an integer part N_i (rounded down) and a fractional part ΔN as shown in Eq. (56).

$$N = N_i + \Delta N \tag{56}$$

Reflected rays are categorised by different orders, where the order n is the number of reflections of a specific ray. The maximum order n_{max} is calculated by Eq. (57) where int is a function which returns the integer part of the argument.

$$n_{\max} = \mathrm{int}\left(\frac{N-1}{4}\right) + 1 \tag{57}$$

Above a certain frequency f_{multi} the contributions from the rays are added according to Eq. (58) and below the frequency according to Eq. (59) (uncorrelated and correlated summation, respectively). The order n of the i'th ray is calculated by Eq. (60) and A_{ray} is calculated by Eq. (61). The plane wave reflection coefficient R is calculated using the grazing reflection angle in Eq. (62).

$$\Delta L_{multi}\left(f \geq f_{multi}\right) = 10\log\left(\left(\Delta N\, R^{n_{\max}}\, A_{ray}\left(n_{\max}\right)\right)^2 + \sum_{i=3}^{N_i}\left(R^n\, A_{ray}\left(n\right)\right)^2\right) \tag{58}$$

$$\Delta L_{multi}\left(f < f_{multi}\right) = 20\log\left(\Delta N\, R^{n_{\max}}\, A_{ray}\left(n_{\max}\right) + \sum_{i=3}^{N_i}\left(R^n\, A_{ray}\left(n\right)\right)\right) \tag{59}$$

$$n = \mathrm{int}\left(\frac{i-1}{4}\right) + 1 \tag{60}$$

$$A_{ray}(n) = 10^{-0.1}\sqrt{\frac{\left|\psi_G - \psi'_G\right|}{\rho_{ray}\sin\psi_G}} \tag{61}$$

where $\rho_{ray} = 0.00001$ and ψ_G and ψ'_G are calculated by Eqs. (62) to (64) respectively.

$$\psi_G = \arccos\left(\frac{C}{c(z_{\max})}\right) \tag{62}$$

$$\psi'_G = \arccos\left(\frac{C}{c(z_{\max}(1+\rho_{ray}))}\right) \tag{63}$$

$$z_{\max} = \frac{d}{n}\sqrt{\frac{A}{2\pi C}} \tag{64}$$

The frequency f_{multi} is determined by Eq. (65) where $i_{multi} = 10\log(f_{multi})$ is the corresponding band number. f_0 (band number i_0) and f_π (band number i_π) is determined on the basis of the terrain effect relative to free field ΔL calculated by the method described in Section 6. f_0 is the smallest one-third octave band centre frequency where ΔL becomes smaller than 0 dB and f_π is the smallest one-third octave band centre frequency where ΔL has a local minimum. The constant i_σ is given by Eq. (66) where σ is the ground flow resistivity.

$$i_{multi} = \text{int}\left(\frac{i_0 + i_\pi}{2}\right) + i_\sigma \tag{65}$$

$$i_\sigma = \begin{cases} 1 & \sigma \le 40000 \\ 0 & 40000 < \sigma < 630000 \\ -1 & \sigma \ge 630000 \end{cases} \tag{66}$$

***Note**: The principle for switching from coherent to incoherent summation at f_{multi} has been developed for flat terrain with a finite impedance where the first dip in the frequency spectrum is well-defined. For other types of terrain especially after the Fresnel-zone interpolation principle has been applied small local minima may occur which can be mistaken for the first dip. In case of screens the ground interference dips are superimposed with the screen attenuation which also will blur the determination of f_{multi}. The difference between coherent and incoherent summation may very well exceed 10 dB at a propagation distance of 1000 m. On the basis of this uncertainty it has been decided to assume incoherent summation in the whole frequency range until a safe principle has been developed for determination of the frequency f_{multi}.*

The method described above is only valid for a logarithmic sound speed profile. However, in [11] a solution has also been given for a linear sound speed profile, but no solution exists for the combination given by Eq. (25). Assuming that the sound speed profile normally will be dominated by the logarithmic term in Eq. (25) a simple modification has been chosen to include the effect of the linear part of the profile. A in Eq. (54) is replaced by a modified value A' calculated by Eq. (67) where $R_{A,B}$ is the radius of curvature for the log-lin sound speed profile defined by the constants A, B, and C. $R_{A,B}$ is calculated by Eqs. (B1) to (B3) shown in Appendix B.

$$A' = \frac{\pi C d^2}{32 R_{A,B}^2} \tag{67}$$

The method described above is valid for a flat terrain with homogeneous surface impedance. If the impedance varies along the propagation path, the average plane wave reflection coefficient R between the source and receiver is used instead.

If the terrain is flat with screens, h_{max} is determined by the maximum value of the source, receiver and screen heights.

If the terrain is non-flat possibly with screens, the heights of source, receiver and screens are determined relative to the terrain baseline and h_{max} is defined as the maximum value of these heights. However, if the average vertical deviation of the terrain from the baseline is less than 0 (meaning that the terrain on average is lower than the baseline indicating a valley shaped terrain), h_{max} is modified by adding the numerical value of the deviation.

***Note**: The proposals for terrain with varying impedances, terrain with screens and non-flat terrain have not been validated and it must be recommended to study this subject more carefully in the future.*

7. Scattering Zones

The calculation of the effect of scattering zones in Section 5 of [4] is based on the sound path length R_{sc} inside the scattering volume. When the line-of-sight is not blocked by obstacles, R_{sc} is measured along the source-receiver sound path and when the line-of-sight is blocked, R_{sc} is measured along the sound path over the top of the obstacles using the "rubber band" principle.

In case of refraction R_{sc} is instead measured along circular rays. When the circular ray used to determine the efficiency of the primary screen edge as described in Section 6.7 is not blocked by a screen R_{sc} is measured along this ray. If this ray is blocked, R_{sc} is instead measured along the circular rays used to determine the efficiency of secondary screens

and edges. The height of the rays at a given propagation distance can be determined using the equations in Appendix B for a log-lin sound speed profile.

In the transition principle described in Section 5.3 of [4] for scattering zones with limited heights the same principle is used except that $z_{ray}(x)$ is the height of the circular ray. If a part of the ray is below the ground surface, the ray is assumed to follow the ground (meaning that $z_{ray}(x)$ can never be less than $z_{ground}(x)$).

8. Reflections

When the propagation path is a path generated by the reflection from an obstacle the direction of propagation before and after the reflection will change relative to the direction of the wind. The implication is that the sound speed profile and consequently the radius of curvature of the circular rays may change at the reflection. If more than one reflection is involved, the curvature of the rays may change each time the ray is reflected. In case of strong sound speed gradients the propagation may involve complicated cases of downward and upward propagation with effects of multiple rays and shadow zones at the same time. The apparently obvious solution is to change the ray curvature piecewise between the points of reflection. However, the geometrical complexity will increase very fast and it has been concluded in [5] that it will not be possible to solve the problem by this approach.

Instead, a simple straightforward, but less physically founded approach has been chosen. The sound speed profile c(z) defined by the parameters A, B and C in Eq. (25) is determined for each straight line segment of the reflected ray path and the average value, weighted by the horizontal length of the path segment d_i, is determined by Eqs. (68) to (70). Then, it is assumed that the effect of refraction can be represented by the average sound speed profile defined by $\overline{A}$, $\overline{B}$ and $\overline{C}$. Figure 13 shows the propagation path in case of a single reflecting surface. If the reflecting surface is close to the source or receiver or if the reflected ray path is close to the direct path, this simple approach is considered reasonable, and in most cases where a reflection is contributing significantly to the sound pressure at the receiver these requirements are fulfilled. However, in cases with downward refraction half the way and upward refraction the rest of the way the approach will lead to a case with no refraction which obviously will be very rough substitution. Fortunately, such cases are of little practical importance unless the direct path is affected by excessive attenuation while the reflected path is not.

$$\overline{A} = \frac{\sum_{i=1}^{n} A_i \, d_i}{\sum_{i=1}^{n} d_i} \tag{68}$$

$$\overline{B} = \frac{\sum_{i=1}^{n} B_i \, d_i}{\sum_{i=1}^{n} d_i} \tag{69}$$

$$\overline{C} = \frac{\sum_{i=1}^{n} C_i \, d_i}{\sum_{i=1}^{n} d_i} \tag{70}$$

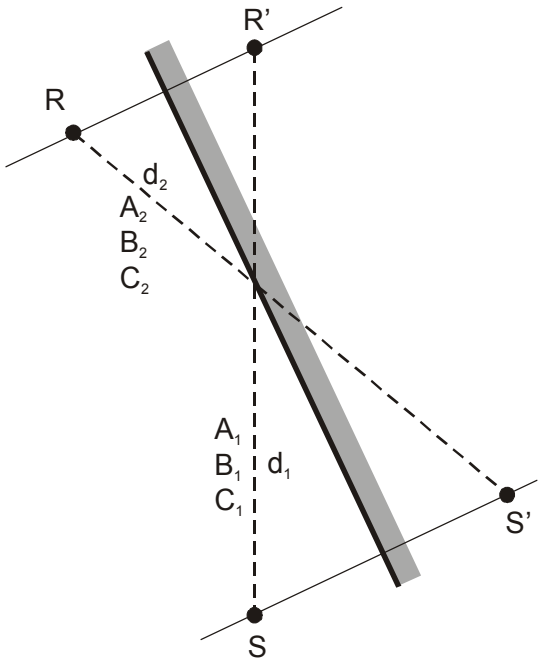

Figure 13
Plan view illustrating different refraction before and after reflection from obstacle.

In the method for an atmosphere without refraction described in [4] the efficiency of reflector due to the size of the reflector is based on the size compared to a Fresnel zone around the reflection point. In case of refraction the same method is used the reflection point shall be determined taking into account that the ray is curved due to refraction. The height of the ray at the reflection point shall be determined using the equations in Appendix B for a log-lin sound speed profile.

9. Conclusions

The comprehensive model for propagation of sound in an atmosphere with moderate refraction described in the present report is based on the model for propagation in an atmosphere without refraction (straight line propagation) described in a companion report. The straight line model is modified to include the effect of atmospheric refraction by introducing circular sound rays. The modification is based on simple equations assuming that the sound speed varies linearly with the height above the ground leading to circular arcs.

Normal “uncomplicated” weather conditions can approximately be represented by a sound speed profile with a logarithmic and a linear part. Therefore, the crux has been to approximate such a non-linear sound speed profile by an equivalent linear profile. A principle has been elaborated which seems to work fairly well for propagation over a flat finite impedance surface.

In case of screens the influence of the screen on the airflow over the screen has only been treated superficially. It is known that the effect of screen-induced wind speed gradients may affect the performance of the screen seriously when the source and the receiver is close to the screen. Therefore, this effect should be investigated more carefully in future.

In case of strong downward refraction the model based on simple geometrical modification of rays has been extended to include the effect of multiple reflections. The objective of the present work has not been to develop a very accurate sound propagation model in cases where the effect of additional rays during strong downward refraction is dominating the overall propagation effect. Still, it is expected that the model for multiple reflection can be improved considerably if more work is carried out in this field.

Also in case of strong upward refraction where no ray will reach the receiver in a shadow zone the model has been extended to include effects of shadow zones. The method that is proposed is not very accurate, but is considered sufficiently accurate for engineering purposes.

In case of reflection from vertical surfaces the sound speed profile may vary along the propagation path because the direction of different parts of the path varies relative to the direction of the wind. A simple principle has been proposed based on the weighted average of the weather conditions of individual path segments. This principle has not been validated and should be studied more closely in future.

10. References

[1] O. M. Arntzen, *A short description of the Matlab functions heurd.m, heurid.m and class2z.m*, SINTEF Report STF40-A99075, Trondheim 1999.

[2] A. L'Espérance, P. Herzog, G. A. Daigle, and J. R. Nicolas, *Heuristic model for outdoor sound propagation based on an extension of the geometrical ray theory in the case of a linear sound speed profile*, Appl. Acoust. 37, 111-139, 1992.

[3] *Numerical Recipes in FORTRAN 77: The Art of Scientific Computing*, Cambridge University Press, ISBN 0-521-43064-X (website http:///www.ulib.org/webRoot/Books/Numerical_Recipes/)

[4] B. Plovsing and J. Kragh, *Nord2000. Comprehensive Outdoor Sound Propagation Model. Part 1: Propagation in an Atmosphere without Significant Refraction*, DELTA Acoustics & Vibration Revised Report AV 1849/00, Hørsholm 2006.

[5] B. Plovsing and J. Kragh, *Comprehensive Model for Sound Propagation - Including Atmospheric Refraction*, DELTA Acoustics & Vibration Report AV 2004/99, Lyngby 1999.

[6] B. Plovsing and J. Kragh, *Approximation of a Non-Linear Sound Speed Profile by an Equivalent Linear Profile*, DELTA Acoustics & Vibration Report AV 2005/99, Lyngby 1999.

[7] E. M. Salomons, *Reduction of the performance of a noise screen due to screen-induced wind speed gradients. Numerical computations and wind tunnel experiments*, J. Acoust. Soc. Am.105, 2287-2293, 1999.

[8] S. Å. Storeheier, *Nord2000: Sound propagation under simplified meteorological models: a heuristic approach*, SINTEF Report STF40 A98075, Trondheim 1998.

[9] S. Å. Storeheier, O. M. Arntzen, *Some effects of using linear sound speed profiles in outdoor sound propagation calculations*. SINTEF Report STF40 A99076, Trondheim 1999.

[10] M. Ögren, *Propagation of Sound - Screening and Ground Effect, Part 2: Refracting Atmosphere*, Swedish National Testing and Research Institute, SP REPORT 1998:40, ISBN: 91-7848-746-3, Borås 1998.

[11] M. Ögren, *Multi reflected rays in a refracting atmosphere - Nord 2000 Progress report*, SP Technical Note 1999:28, Borås 1999.

[12] R. Nota, R. Barelds, D. van Maercke, *Harmonoise WP3 engineering method for road traffic and railway noise after validation and fine-tuning*, Technical Report HAR32TR-040922-DGMR20, 2005.

[13] R. Eurasto, *Nord2000 for road traffic noise prediction. WP4: Weather classes and statistics*, VTT Report VTT-R-02530-06, Espoo 2006

Appendix A

Determination of the Height at a Circular Ray

The geometrical parameters for a circular ray between point 1 at $(0,h_1)$ and point 2 at (d,h_2) at a relative sound speed gradient ξ are defined in Figure A1. The purpose of the solution described below is to determine the height h_0 of the ray corresponding to the horizontal distance d_0.

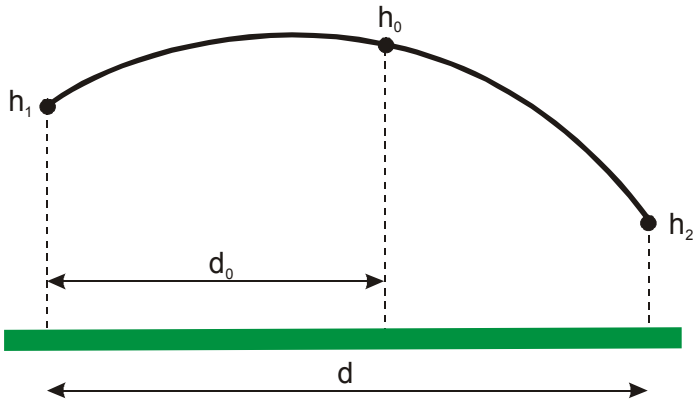

Figure A1
The geometrical parameters for a circular ray used to calculate the height on a point on the ray.

In order to normalize the problem to the solution given in Section 2, the parameters ξ', d_0', h_1' and Δh are defined as shown in Eqs. (A1) to (A6).

$$\xi' = |\xi| \tag{A1}$$

$$\Delta h = |h_1 - h_2| \tag{A2}$$

$$\xi > 0 \wedge h_1 > h_2 : \quad h_1' = h_2, \quad d_0' = d - d_0 \tag{A3}$$

$$\xi > 0 \wedge h_1 \le h_2 : \quad h_1' = h_1, \quad d_0' = d_0 \tag{A4}$$

$$\xi < 0 \wedge h_1 \ge h_2 : \quad h_1' = -h_1, \quad d_0' = d_0 \tag{A5}$$

$$\xi < 0 \wedge h_1 < h_2 : \quad h_1' = -h_2, \quad d_0' = d - d_0 \tag{A6}$$

Now the height h_0 can be determined by Eqs. (A7) to (A12) where sign(x) is the signum function. (x_0,z_0) is the centre of circular ray.

$$\tan\psi = \frac{\xi' d}{2} + \frac{\Delta h\left(2 + \xi' \Delta h\right)}{2d} \tag{A7}$$

$$x_0 = \frac{\tan\psi}{\xi'} \tag{A8}$$

$$z_0 = h_1^{'} - \frac{1}{\xi'} \tag{A9}$$

$$R = \frac{1}{\xi' \cos(\psi)} \tag{A10}$$

$$\theta = \arccos\left(\frac{d_0^{'} - x_0}{R}\right) \tag{A11}$$

$$h_0 = sign(\xi)\left(R\sin(\theta) + z_0\right) \tag{A12}$$

Appendix B

Determination of the Ray Height in Case of a Log-Lin Sound Speed Profile

During the revision of the Nord2000 method it has been considered if the principles for determining ray curvature in the Harmonoise engineering model for road traffic and railway noise could provide better results than obtained by the principles developed in the Nord2000 work. It was found that the prediction of the travel time differences essential to ground effects and the prediction of diffraction angles essential to screening effects were not improved by using the Harmonoise method. However, it was found that the Harmonoise method predicts a more realistic ray path compared to the Nord2000 method. Therefore, in the parts of the Nord2000 method where the position of the ray path is important and where the height of the ray has to be determined it is better to use the Harmonoise method.

This appendix describes how the height of the ray is determined using the Harmonoise ray curvature equations in case of the log-lin sound speed profile defined in Eq. (24) in Section 3. The radius of curvatures R_A and R_B of the logarithmic and linear part of the sound speed profile is calculated by Eqs. (B1) and (B2), respectively and the combined radius $R_{A,B}$ by Eq. (3). A, B, C are the weather constants in Eq. (24) and d is the horizontal distance.

$$R_A = sign(A)\frac{d}{8}\sqrt{\frac{2\pi C}{|A|}} \tag{B1}$$

$$R_B = sign(B)\sqrt{\left(\frac{C}{|B|}\right)^2 + \left(\frac{d}{2}\right)^2} \tag{B2}$$

$$R_{A,B} = \frac{1}{\frac{1}{R_A} + \frac{1}{R_B}} \tag{B3}$$

The relative gradient ξ_{ray} of the equivalent sound speed profile used to determine the approximate ray path is calculated by Eq. (B4) where ψ_S is the start angle of the ray given by Eq. (B5).

$$\xi_{ray} = \frac{1}{R_{A,B}\cos(\psi_S)} \tag{B4}$$

$$\psi_S = \arcsin\left(\frac{\sqrt{d^2 + (h_R - h_S)^2}}{2R_{A,B}}\right) + \arctan\left(\frac{h_R - h_S}{d}\right) \qquad \text{(B5)}$$

The height of the ray along the propagation path can now be determined using the equations given in Appendix A and the relative sound speed gradient given by Eq. (B4).

Appendix C

Propagation Effect of a Finite Impedance Wedge in Case of Refraction

The refraction-modified geometrical parameters used in the diffraction solution for a finite impedance wedge is shown in Figure B1. In the presentation of the solution shown in the following it is assumed that $0 \le \theta_R \le \theta_S \le \beta \le 2\pi$. If this is not the case, the angles have to be modified as described at the end of this appendix.

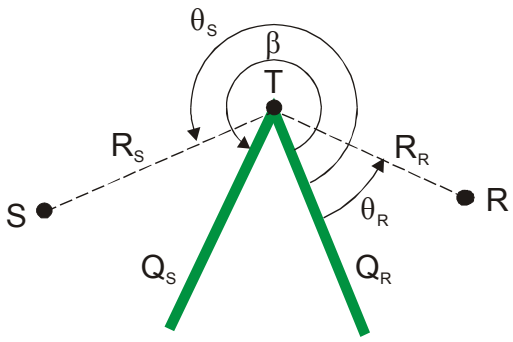

Figure B1
Definition of refraction-modified parameters for calculation of the propagation effect of a wedge-shaped screen with finite surface impedance.

The wedge solution is shown in Eq. C1. p_{diffr} is the diffracted sound pressure, ω is the angular frequency ($=2\pi f$), τ is the total travel time along the diffracted path ($\tau = \tau_S + \tau_R$) and P is the length of the diffracted path ($P = R_S + R_R$).

$$p_{diffr} = -\frac{1}{\pi}\sum_{n=1}^{4} Q_n A(\theta_n) E_v\left(A(\theta_n)\right)\frac{e^{j\omega\tau}}{\ell} \qquad \text{(C1)}$$

The angle θ_n is defined by

$\theta_1 = \theta_S - \theta_R$

$\theta_2 = \theta_R + \theta_S$

$\theta_3 = 2\beta - (\theta_R + \theta_S)$

$\theta_4 = 2\beta - (\theta_S - \theta_R)|$

The "reflection coefficient" Q_n is given by

$Q_1 = 1$

$Q_2 = Q_R$

$Q_3 = Q_S$

$Q_4 = Q_S Q_R$

Q_S is calculated using P as the distance parameter and $\psi_G = \beta - \theta_S$ as the grazing angle. Q_R is calculated using P as the distance parameter and $\psi_G = \theta_R$ as the grazing angle. If ψ_G becomes greater than $\pi/2$, $\psi_G = \pi/2$ is used instead.

$E_\nu(A(\theta_n))$ is calculated by Eq. (C2) where $\nu = \pi/\beta$ is the wedge index. The solution is only valid for wedge angles greater than π.

$$E_\nu\left(A(\theta_n)\right) = \frac{\pi}{\sqrt{2}} \frac{\sin\left|A(\theta_n)\right|}{\left|A(\theta_n)\right|} \frac{e^{j\pi/4}}{\sqrt{1 + \left(\frac{2\tau_S\tau_R}{\tau^2} + \frac{1}{2}\right)\frac{\cos^2\left|A(\theta_n)\right|}{\nu^2}}} A_D(B) \qquad \text{(C2)}$$

In the equation $A(\theta_n)$ is given by Eq. (C3), B by Eq. (C4) and $A_D(B)$ by Eq. (C5). H(x) is Heavisides' step function (H = 1 for $x \geq 0$ and H = 0 for $x < 0$).

$$A(\theta_n) = \frac{\nu}{2}\left(-\beta - \pi + \theta_n\right) + \pi H\left(\pi - \theta_n\right) \qquad \text{(C3)}$$

$$B = \sqrt{\frac{4\omega\tau_S\tau_R}{\pi\tau}} \frac{\cos\left|A(\theta_n)\right|}{\sqrt{\nu^2 + \left(\frac{2\tau_S\tau_R}{\tau^2} + \frac{1}{2}\right)\cos^2\left|A(\theta_n)\right|}} \qquad \text{(C4)}$$

$$A_D(B) = sign(B)\left(f\left(|B|\right) - jg\left(|B|\right)\right) \qquad \text{(C5)}$$

In Eq. (C5) sign(x) is the signum function (sign = 1 for $x > 0$, sign = 0 for $x = 0$, sign = -1 for $x < 0$). f(x) and g(x) are the auxiliary Fresnel functions. If $x \geq 5$, f(x) and g(x) are calculated by Eqs. (C6) and (C7). If $0 < x < 5$, f(x) is calculated by the polynomial fit in Eq. (C8). The constants a_0 to a_{12} are defined in Table C1. A similar polynomial fit is used to calculate g(x) using the constants a_0 to a_{12} defined in Table C2.

$$f(x) = \frac{1}{\pi x} \qquad \text{(C6)}$$

$$g(x) = \frac{1}{\pi^2 x^3} \tag{C7}$$

$$f(x) = \sum_{n=0}^{12} a_n x^n \tag{C8}$$

a_{12}	0.00000019048125
a_{11}	-0.00000418231569
a_{10}	0.00002262763737
a_9	0.00023357512010
a_8	-0.00447236493671
a_7	0.03357197760359
a_6	-0.15130803310630
a_5	0.44933436012454
a_4	-0.89550049255859
a_3	1.15348730691625
a_2	-0.80731059547652
a_1	0.00185249867385
a_0	0.49997531354311

Table C1
Constants in polynomial fit of f(x) for 0 < x < 5.

a_{12}	-0.00000151974284
a_{11}	0.00005018358067
a_{10}	-0.00073624261723
a_9	0.00631958394266
a_8	-0.03513592318103
a_7	0.13198388204736
a_6	-0.33675804584105
a_5	0.55984929401694
a_4	-0.50298686904881
a_3	-0.06004025873978
a_2	0.80070190014386
a_1	-1.00151717179967
a_0	0.50002414586702

Table C2
Constants in polynomial fit of g(x) for 0 < x < 5.

If the wedge edge is below the line from the source to the receiver ($\theta_1 < \pi$), the contribution from the direct ray shall be added to the solution as shown in Eq. (C9). R_1 and τ_1 which is the distance and travel time between the source and receiver are calculated by Eqs. (C10) and (C11).

$$p = p_{diffr} + \frac{e^{j\omega\tau_1}}{R_1} \tag{C9}$$

$$R_1 = \sqrt{R_S^2 + R_R^2 - 2R_S R_R \cos(\theta_1)} \tag{C10}$$

$$\tau_1 = \sqrt{\tau_S^2 + \tau_R^2 - 2\tau_S \tau_R \cos(\theta_1)} \tag{C11}$$

If the wedge edge is below the line from the source to the image receiver ($\theta_2 < \pi$), the contributions from the direct ray as well as the ray reflected in the receiver face of the wedge shall be added to the solution as shown in Eq. (C11). R_2 and τ_2 which is the distance and travel time between the source and image receiver are calculated by Eqs. (C13) and (C14). Q_R is the reflection coefficient calculated on the basis of R_2 and $\psi_{G,R}$ determined by Eq. (C15).

$$p = p_{diffr} + \frac{e^{j\omega\tau_1}}{R_1} + Q_R \frac{e^{j\omega\tau_2}}{R_2} \tag{C12}$$

$$R_2 = \sqrt{R_S^2 + R_R^2 - 2R_S R_R \cos(\theta_2)} \tag{C13}$$

$$\tau_2 = \sqrt{\tau_S^2 + \tau_R^2 - 2\tau_S \tau_R \cos(\theta_2)} \tag{C14}$$

$$\psi_{G,R} = \arcsin\left(\frac{R_S \sin\theta_S + R_R \sin\theta_R}{R_2}\right) \tag{C15}$$

If the wedge edge is below the line from the image source to the receiver ($\theta_3 < \pi$), the contributions from the direct ray as well as the ray reflected in the source face of the wedge shall be added to the solution as shown in Eq. (C16). R_3 and τ_3 which is the distance and travel time between the image source and receiver are calculated by Eqs. (C17) and (C18). Q_S is the reflection coefficient calculated on the basis of R_3 and $\psi_{G,S}$ determined by Eq. (C19).

$$p = p_{diffr} + \frac{e^{j\omega\tau_1}}{R_1} + Q_S \frac{e^{j\omega\tau_3}}{R_3} \tag{C16}$$

$$R_3 = \sqrt{R_S^2 + R_R^2 - 2R_S R_R \cos(\theta_3)} \tag{C17}$$

$$\tau_3 = \sqrt{\tau_S^2 + \tau_R^2 - 2\tau_S \tau_R \cos(\theta_3)} \tag{C18}$$

$$\psi_{G,S} = \arcsin\left(\frac{R_S \sin(\beta - \theta_S) + R_R \sin(\beta - \theta_R)}{R_3}\right) \tag{C19}$$

If $\theta_n = \pi$, numerical problems will occur when calculating the diffracted sound pressure according to Eq. (C1). This can be fixed by subtracting a small quantity ε from θ_n when $|\theta_n - \pi| < \varepsilon$. $\varepsilon = 10^{-8}$ has been found suitable, but may depend on the implementation.

In cases where the source and receiver are reflected by a ground surface before and after the wedge the calculation will also be carried out for the image source and receiver as described in [4] in Sections 4.4.3.4 and 4.4.3.5. In such cases the “source” or “receiver” may be inside the wedge. The same may happen when for the source and receiver in case of upward refraction. This is in both cases taken care of by modifying the angles according to the following scheme where θ'_R, θ'_S andβ' are the modified angles.

$0 > \theta_R > \beta - 2\pi$:

$\theta'_R = 0$

$\theta'_S = \theta_S - \theta_R$

$\beta' = \beta - \theta_R$

$\theta_R \leq \beta - 2\pi$:

$\theta'_R = 0$

$\theta'_S = 2\pi-(\beta - \theta_S)$

$\beta' = 2\pi$

$\beta < \theta_S < 2\pi$ (θ'_S and β' are used instead when modified above):

$\beta' = \theta_S$

$\theta_S \geq 2\pi$ (θ'_S is used instead when modified above):

$\theta'_S = 2\pi$

$\beta' = 2\pi$